

here the number of possible Kekulé structures grows exponentially with chain length.<sup>23</sup> Recent calculations show that long-chain polymers of this family should be significantly stable,<sup>22,23</sup> and recent experimental work, though not fully characterizing the products, indicates that wider polymers of this family may exist.<sup>27</sup> The last group of molecules in Table IV compares several fragments which can be cut from the graphite (infinite 2-dimensional hexagonal) lattice. Those fragments identified with an asterisk can be shown to provide upper bounds to the energy per site of graphite<sup>28</sup> since they can be repeated to cover the whole lattice. The most stable fragments seem to be those having the highest proportion of corrugated (polyphenanthrene-like) edge and the least zigzag (polyacene-like) edge. This may be related to the way in which edge erosion occurs in graphite.<sup>26,29</sup>

The results for our two largest molecules, coronene and dibenz[fg,op]naphthacene, give us a chance to compare two "rules of thumb" for estimating the stability of conjugated benzenoid hydrocarbons. One rule states simply that the maximum stability for molecules with a given number of carbon atoms is attained when the perimeter of the molecule is minimized (i.e., when the H/C ratio is minimized).<sup>30</sup> For 24 carbon atoms the minimum

perimeter is that of coronene. On the other hand, the ideas of Clar<sup>31</sup> lead one to conclude that the most stable molecules will be those which are most fully "benzenoid" (i.e., for which one can draw Clar structures with as many circles as possible). For 24 carbon atoms this rule predicts dibenz[fg,op]naphthacene (4 circles) to be more stable than coronene (3 circles).<sup>32</sup> In this view the central hexagon of coronene is essentially a hole which does not contribute to the aromaticity. As can be seen from Tables II and IV, both the raw valence bond energies and the Dewar-type aromatic stabilization energies here favor the minimum perimeter rule. In fact, the computed VB energy of coronene currently provides the best rigorous upper bound to the VB energy of the graphite lattice.<sup>28</sup>

**Acknowledgment.** We thank Florida State University for providing us with a grant of computer time on their Cyber 205. Special thanks also go to Dr. Kenneth Flurchick of ETA Systems, Inc. for his assistance with the coronene calculation.

**Registry No.** Benzene, 71-43-2; naphthalene, 91-20-3; biphenyl, 92-52-4; anthracene, 120-12-7; phenanthrene, 85-01-8; stilbene, 588-59-0; pyrene, 129-00-0; naphthacene, 92-24-0; benz[a]anthracene, 56-55-3; benzophenanthrene, 65777-08-4; chrysene, 218-01-9; triphenylene, 217-59-4; *p*-terphenyl, 92-94-4; *m*-terphenyl, 92-06-8; *o*-terphenyl, 84-15-1; perylene, 198-55-0; benz[a]pyrene, 50-32-8; benz[e]pyrene, 192-97-2; pentacene, 135-48-8; picene, 213-46-7; benz[b,cd]pyrene, 191-26-4; benz[ghi]perylene, 191-24-2; dibenzol[fg,op]naphthacene, 192-51-8; coronene, 191-07-1.

(27) (a) Murakami, M.; Yoshimura, S. *J. Chem. Soc., Chem. Commun.* **1984**, 1649. (b) Murakami, M.; Yoshimura, S. *Mol. Cryst. Liq. Cryst.* **1985**, *118*, 95.

(28) Klein, D. J.; Alexander, S. A.; Seitz, W. A.; Schmalz, T. G.; and Hite, G. E. *Theor. Chim. Acta* **1986**, *69*, 393.

(29) Note the important difference between oxidizing and reducing environments. See: (a) Wong, C.; Yang, R. T.; Halpern, B. L. *J. Chem. Phys.* **1983**, *78*, 3325. (b) Mims, C. A.; Chludzinski, J. J., Jr.; Pabst, J. K.; Baker, J. *Catal.* **1984**, *88*, 98. (c) Thomas, J. M. In *Chemistry and Physics of Carbon*; Walker, P. L., Jr., Ed.; Dekker: New York, 1965; Vol. 1.

(30) See, for example: Stein, S. E. *J. Phys. Chem.* **1978**, *82*, 566.

(31) Clar, E. *The Aromatic Sextet*; John Wiley and Sons: London, 1972.

(32) Dias, J. R. *Acc. Chem. Res.* **1985**, *18*, 241.

## Cycloalkylmethyl Radicals. 5. 6- to 15-Membered Rings: EPR Studies of Ring Conformations and Stereodynamics<sup>1</sup>

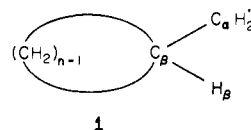
K. U. Ingold\*<sup>2</sup> and J. C. Walton\*<sup>3</sup>

Contribution from the Division of Chemistry, National Research Council of Canada, Ottawa, Ontario K1A 0R6, Canada, and Department of Chemistry, The University, St. Andrews, Fife, Scotland KY16 9ST, U.K. Received November 12, 1986

**Abstract:** Cycloalkylmethyl radicals having 7- to 15-membered rings (excluding cyclotetradecylmethyl) have been generated and examined by EPR spectroscopy. All the cycloalkylmethyl radicals from the 9-membered ring upward show two distinguishable conformers, though there may be additional conformers present with cyclodecylmethyl and cyclopentadecylmethyl radicals. All the cycloalkylmethyl radicals from the 10-membered ring upward have one conformer, the quasi-equatorial, QE, with an  $H_\beta$  hfs in the range 27.7–32.0 G at 140 K and one conformer, the quasi-axial, QA, with an  $H_\beta$  hfs in the range 38.3–40.4 G at 140 K. The QE and QA conformers have been assigned to species in which the  $CH_2^*$  group occupies "outer-edge" and "corner" sites, respectively, in the preferred conformations of the cycloalkanes. The EPR results indicated that the preferred conformations of the  $C_9$ ,  $C_{10}$ ,  $C_{11}$ ,  $C_{12}$ ,  $C_{13}$ , and  $C_{15}$  rings were [333], [2323], [335], [3333], [346], and [33333], respectively. Arrhenius parameters for ring-atom site exchange in the cycloalkylmethyl radicals have been determined from the exchange broadening in the EPR spectra. These EPR barriers are compared with literature data on cycloalkane free energy barriers measured by NMR and enthalpic barriers estimated by force field and related methods.

The  $C_\alpha H_2^*$  group in cycloalkylmethyl radicals, **1**, provides a novel and useful conformational "spin probe" that can be monitored by EPR spectroscopy.<sup>4-7</sup> This probe yields both the pre-

ferred conformation of the  $C_\alpha H_2^*$  group with respect to the  $C_\beta-H_\beta$  bond and, more interestingly, information regarding ring conformations and even, in suitable cases, information regarding the dynamics of interconversion of ring conformers. For example,



**1**

both the cyclohexylmethyl radical and the *cis*-(4-methylcyclohexyl)methyl radical exist as mixtures of two conformers, one

(1) Issued as NRCC No. 27590. Part 4: Reference 4.

(2) NRCC.

(3) The University, St. Andrews.

(4) Walton, J. C. *J. Chem. Soc., Perkin Trans. 2* **1986**, 1641-1646.

(5) Ingold, K. U.; Walton, J. C. *J. Am. Chem. Soc.* **1985**, *107*, 6315-6317.

(6) Ingold, K. U.; Walton, J. C. *J. Chem. Soc., Perkin Trans. 2* **1986**, 1337-1344.

(7) Kemball, M. L.; Walton, J. C.; Ingold, K. U. *J. Chem. Soc., Perkin Trans. 2* **1982**, 1017-1023.

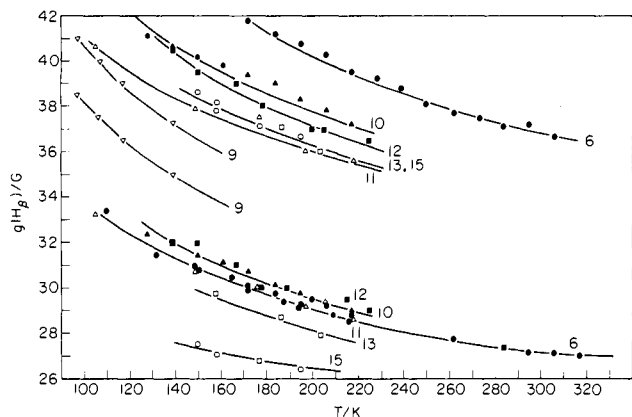


**Figure 1.** Values of  $a^{H_\beta}$  as a function of temperature for **1**. Key:  $n = 6$ ,  $\bullet$ ;  $n = 9$ ,  $\nabla$ ;  $n = 10$ ,  $\blacktriangle$ ;  $n = 11$ ,  $\triangle$ ;  $n = 12$ ,  $\blacksquare$ ;  $n = 13$ ,  $\square$ ;  $n = 15$ ,  $\circ$ . The upper curves correspond to the quasi-axial, QA, and the lower to the quasi-equatorial, QE, radical conformers.

having  $\text{CH}_2^*$  axial and one having  $\text{CH}_2^*$  equatorial.<sup>5,6</sup> From quantitative measurements of the concentrations of the axial and equatorial conformers over a range of temperatures, the conformational enthalpic and entropic axial/equatorial preference of the  $\text{CH}_2^*$  group on a 6-membered ring was determined.<sup>5,6</sup> Furthermore, for the *cis*-(4-methylcyclohexyl)methyl radical the dynamics of the cyclohexane ring inversion were determined.<sup>6</sup> The  $\text{CH}_2^*$  group has proved equally useful in determining the conformational preferences and equilibria of the cyclohex-2-enylmethyl and cyclohex-3-enylmethyl radicals.<sup>4</sup>

NMR spectroscopy has, of course, been extremely successful in defining the conformational preferences and equilibria of cyclohexane and its derivatives but has proved to be less useful with larger rings. This is due to two factors. First, the barriers to conformational interconversion of the larger rings are considerably lower than the barriers in cyclohexanes. It is therefore difficult to "freeze-out" the motions of larger rings on the NMR time scale. Second, the actual equilibria are complex, and if, in addition, the symmetry is low, then very complex NMR spectra are obtained. For these reasons, there have been comparatively few NMR studies of the larger cycloalkanes and the interpretation of the results has been difficult and not infrequently rather inconclusive.

As we have previously reported,<sup>7</sup> the cycloundecylmethyl radical, **1** ( $n = 11$ ), exists in two distinct forms at temperatures  $< 230$  K; these forms interconvert rapidly on the EPR time scale at higher temperatures. The main spectroscopic difference between these two radicals lies in the magnitudes of their  $H_\beta$  hyperfine splittings (hfs); at 140 K one radical has  $a^{H_\beta} = 38.3$  G, and the other,  $a^{H_\beta} = 31.1$  G. It therefore seemed probable to us that other **1** with  $n \geq 6$  might give EPR spectra showing the presence of more than one conformer. Such proved to be the case for **1** ( $n = 9-13, 15$ ),<sup>8</sup> as we report herein, but not for **1** ( $n = 7$ )<sup>9</sup> nor for **1** ( $n = 8$ ).<sup>7</sup> Our conclusions are compared with what little information is available on the larger cycloalkanes from studies by NMR, by X-ray diffraction, and by force field and other theoretical treatments.

## Results

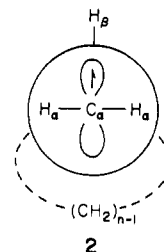
The cycloalkylmethyl radicals, **1**, were formed by bromine atom abstraction from the corresponding bromides with photochemically generated triethylsilyl or trimethyltin radicals in *tert*-butylbenzene at  $T \geq 200$  K and in cyclopropane or propane at lower temperatures. The EPR parameters for the radicals observed at 140 K (which were confirmed by spectral simulation) are given in Table I. The  $H_\beta$  hfs all showed negative temperature coefficients; i.e.,  $a^{H_\beta}$  decreased with increasing temperature (see Figure 1). This indicates that in all these radicals the preferred conformation about

**Table I.** Hydrogen Hfs (in Gauss) of Cycloalkylmethyl Radicals at 140 K

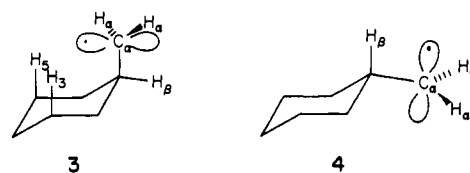
ring size $n$	conform <sup>a</sup>	$a^{H_\alpha}$ (2 H)	$a^{H_\beta}$ (H)	$a^H$ (other)
6	axial, <b>3</b> <sup>b</sup>	22.1	42.4	0.75 (5 H)
	equatorial, <b>4</b> <sup>b</sup>	22.2	30.7	0.95 (4 H)
7		22.1	37.6	
8		21.6	40.1	0.8 (4 H)
9	QA	22.3	37.2	0.8 (4 H)
	QE	22.3	~35.0	
10	QA	22.3	40.5	
	QE <sup>c</sup>	22.3	31.9	
11	QA	21.4	38.3	
	QE	21.4	31.1	
12	QA	22.0	40.5	
	QE	22.0	32.0	
13	QA	22.2	39.3	
	QE	22.2	30.4	
15	QA	22.0	39.3	
	QE <sup>c</sup>	22.0	27.7	

<sup>a</sup>QA = quasi-axial; QE = quasi-equatorial. <sup>b</sup>Data are for the *cis*-(4-methylcyclohexyl)methyl radical because the axial conformer of cyclohexylmethyl is present at too low a concentration to be detected at 140 K.<sup>5,6</sup> <sup>c</sup>There may be two QE conformers (see text).

the  $\text{C}_\beta\text{-C}_\alpha^*$  bond is one in which the  $\text{C}_\alpha$   $2p_z$  orbital (i.e., the SOMO) eclipses the  $\text{C}_\beta\text{-H}_\beta$  bond, i.e., **2**.



We have shown previously<sup>5,6</sup> that two conformers of the cyclohexylmethyl radical can be observed: The one with the larger  $a^{H_\beta}$  has the  $\text{CH}_2^*$  group axial, and that with the smaller  $a^{H_\beta}$  has this group equatorial. The different magnitudes of the  $H_\beta$  hfs arise because the barrier to rotation about the  $\text{C}_\beta\text{-C}_\alpha^*$  bond is considerably higher in the axial conformer, **3** (because of steric interactions between  $\text{H}_\alpha$  and  $\text{H}_3, \text{H}_5$  during rotation), than in the equatorial conformer, **4**. The axial radical, **3**, therefore has a



stronger preference for conformation **2** than does the equatorial radical, **4** and this is reflected by a larger  $H_\beta$  hfs because orbital overlap between the SOMO and the  $\text{C}_\beta\text{-H}_\beta$  bond is enhanced.

The results of Table I are remarkable in that *all* cycloalkylmethyl radicals having  $n \geq 9$  are present in two and only two readily distinguishable conformations despite the fact that a considerable number of conformations are, in principle, possible for such large rings. Those **1** having  $n \geq 10$  have one conformer with a small  $H_\beta$  hfs (27.7–32.0 G at 140 K) and one with a larger  $H_\beta$  hfs (38.3–40.4 G at 140 K). By analogy with **1** ( $n = 6$ ) we classify the smaller  $H_\beta$  hfs conformers as quasi-equatorial, QE, and the larger  $H_\beta$  hfs conformers as quasi-axial, QA. Furthermore, we conclude that the barrier to rotation of the  $\text{CH}_2^*$  group is greater in the QA than in the QE conformation.

**1** ( $n = 6-8$ ). Our studies on **1** ( $n = 6$ ) and on *cis*- and *trans*-(4-alkylcyclohexyl)methyl radicals have already been reported in some detail.<sup>5,6</sup> We include data on **1** ( $n = 6$ ) merely for comparative purposes. The same is true for **1** ( $n = 7$ ).<sup>9</sup> We previously reported that **1** ( $n = 8$ ) exists as only one conformer.<sup>7</sup> In view of our present results with larger rings, this seemed rather

(8) And, of course, for  $n = 6$ , see ref 5 and 6. We have not yet examined **1** ( $n = 14$ ).

(9) Walton, J. C., unpublished results.

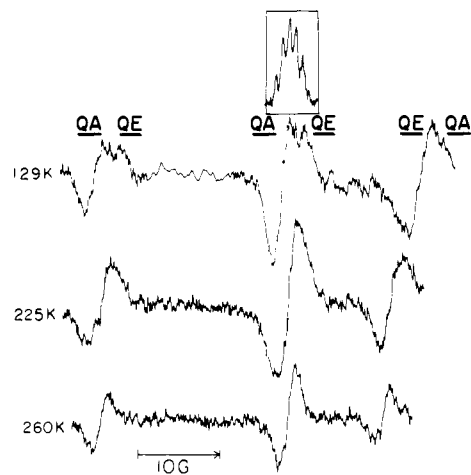


Figure 2. EPR spectra (low-field halves, 9.4 GHz) of **1** ( $n = 9$ ) in cyclopropane at various temperatures. The inset shows the central line ( $m_B = -1/2$ ,  $m_A = 0$ ) at high resolution as a second-derivative presentation. QA and QE refer to quasi-axial and quasi-equatorial conformers, respectively.

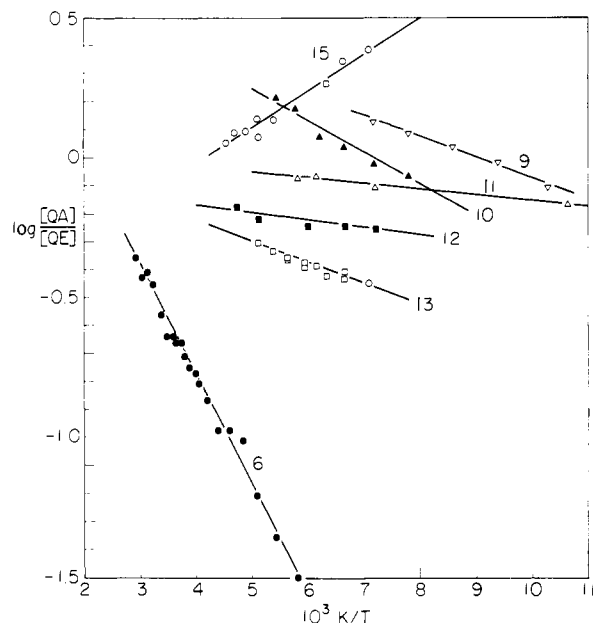


Figure 3. Plots of  $\log([QA]/[QE])$  vs  $10^3 K/T$  for **1**. Key:  $n = 6$ , ●;  $n = 9$ , ▽;  $n = 10$ , ▲;  $n = 11$ , △;  $n = 12$ , ■;  $n = 13$ , □;  $n = 15$ , ○.

surprising, particularly since the barrier to ring inversion of cyclooctane is ca. 7–8 kcal/mol, according to NMR measurements.<sup>10,11</sup> Such a barrier should make the slow-exchange limit for conformational interconversion of cyclooctylmethyl radicals readily accessible in the temperature range of our EPR studies. Nevertheless, upon reexamining this radical, we could still detect only a single conformer in the temperature range 110–270 K. From the signal/noise ratio at 210 K we estimate that the concentration of any other conformer must be <10% of that of the observed species.<sup>12</sup>

**1** ( $n = 9$ ). At low temperatures this radical exists in two conformations (see Figure 2); their relative concentrations (determined by spectral simulation) between 100 and 140 K are plotted as  $\log([QA]/[QE])$  vs  $1/T$  in Figure 3. It can be seen

(10) Anet, F. A. L.; Hartman, J. S. *J. Am. Chem. Soc.* **1963**, *85*, 1204–1205. Anet, F. A. L.; St. Jacques, M. *ibid.* **1966**, *88*, 2585–2586 and 2586–2587.

(11) Anet, F. A. L.; Anet, R. In *Dynamic Nuclear Magnetic Resonance Spectroscopy*; Jackman, L. M., Cotton, F. A., Eds.; Academic: New York, 1975; Chapter 14, pp 543.

(12) In view of the fine structure that is observable<sup>7</sup> in the spectrum of **1** ( $n = 8$ ) (see Table I), we consider it unlikely that a second conformer has an EPR spectrum that “accidentally” coincides with that of the main conformer.

Table II. Van't Hoff Parameters for the QA and QE Equilibria<sup>a</sup>

ring size $n$	$\Delta S^\circ$ , Gibbs/mol	$\Delta H^\circ$ , kcal/mol	$\Delta G^\circ_{300K}$ , kcal/mol
6	$3.6 \pm 0.5$	$1.79 \pm 0.04$	-0.71
9	$2.9 \pm 0.5$	$0.32 \pm 0.02$	0.55
10	$4.0 \pm 0.2$	$0.56 \pm 0.06$	0.64
11	$0.1 \pm 0.03$	$0.09 \pm 0.01$	-0.06
12	$-0.2 \pm 0.03$	$0.14 \pm 0.02$	-0.20
13	$0.1 \pm 0.02$	$0.31 \pm 0.02$	-0.28
15	$-2.5 \pm 0.1$	$-0.58 \pm 0.05$	-0.17

<sup>a</sup> Calculated from the [QA]:[QE] ratios presented in Figure 3. The data for **1** ( $n = 6$ ) have been given previously.<sup>5,6</sup>

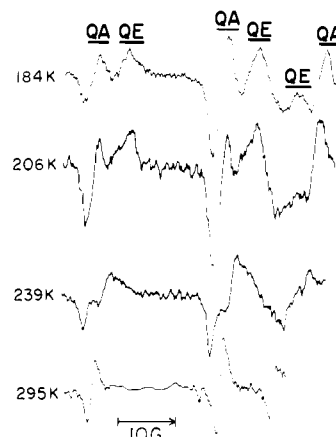


Figure 4. EPR spectra (low-field halves, 9.4 GHz) of **1** ( $n = 10$ ) in *tert*-butylbenzene at various temperatures.

that the quasi-equatorial, QE, conformer predominates for  $T < 110$  K and the quasi-axial, QA, conformer at higher temperatures. At 150 K the QA conformer shows fine structure with hfs by four equivalent  $\gamma$ -hydrogens (see inset in Figure 2). No fine structure could be resolved in the QE conformer's spectrum nor in the spectrum of any **1** ( $n > 9$ ). The van't Hoff parameters for the QA  $\rightleftharpoons$  QE equilibrium, derived from the variation in the [QA]/[QE] ratio with temperature, are given in Table II. Error limits are rather large because of relatively poor resolution of the QA and QE spectra. The EPR spectra showed line broadening between 180 and 260 K, sharpening at the latter temperature to give a single averaged spectrum with  $a^{\text{H}_\alpha}$  (2 H) = 22.2 G and  $a^{\text{H}_\beta}$  (1 H) = 33.3 G (see Figure 2). The exchange-broadened spectra were simulated<sup>13</sup> with a two-jump model, the relative concentrations of QA and QE being obtained by extrapolation of the low-temperature data. Arrhenius parameters for the forward and reverse processes, defined in eq 1, are given in Table III. These



parameters are less precise than we would wish because rather poor spectral resolution produces a certain “softness” in the fits of calculated and experimental spectra.

**1** ( $n = 10$ ). The QA and QE radicals have well-resolved spectra (Figure 4), and a plot of  $\log([QA]/[QE])$  vs  $1/T$  is shown in Figure 3, with the derived van't Hoff parameters given in Table II. Attempts to simulate the exchange broadening that is observed from 190 to 260 K using a two-jump model were rather unsatisfactory. Indeed, the spectra suggest that there are two separate exchange processes that are partly temperature resolved.<sup>14</sup> That is, the lines from the QA conformer remain sharp while the QE lines start to broaden (see Figure 4). On this basis, plus the fact that even at low temperatures the line width for the QE radical is greater (2.0 G) than that for most **1** (ca. 1.6 G), we consider it probable that the QE spectrum is actually due to two spectrally unresolved QE conformers. Proper simulation would require a

(13) Heinzer, J. *QCPE* **1972**, No. 209.

(14) For another example of this very rare phenomenon see: Ingold, K. U.; Nonhebel, D. C.; Walton, J. C. *J. Phys. Chem.* **1985**, *89*, 4424–4426.

**Table III.** Coalescence Temperatures ( $T_c$ ) and Arrhenius Parameters for the Ring-Atom Site Exchange for Cycloalkylmethyl Radicals Calculated by Matching Experimental and Simulated Spectra Plus Cycloalkane Free Energy Barriers for Site Exchange Measured by NMR and Enthalpic Barriers Estimated by Various Methods

ring size $n$	$T_c$ , K	$T$ range, <sup>a</sup> K	$\log A_f$ , <sup>b</sup> s <sup>-1</sup>	$\log A_b$ , <sup>b</sup> s <sup>-1</sup>	$E_f$ , <sup>b</sup> kcal/mol	$E_b$ , <sup>b</sup> kcal/mol	$\Delta G^*$ , <sup>c</sup> kcal/mol	$\Delta H_f$ , <sup>d</sup> kcal/mol	$E_{\Delta}$ , <sup>e</sup> kcal/mol
6			$13.3 \pm 1.0^f$	$14.7 \pm 1.0^f$	$9.0 \pm 1.0^f$	$10.1 \pm 1.0^f$	10.5		$10.9^g, 10.5^h$
9	~220	180–260	$11.8 \pm 1.0$	$12.5 \pm 1.0$	$5.4 \pm 0.2$	$5.7 \pm 0.2$	~6	8.6	$7.7^i, 7.0^j$
10	230	190–290			~6	~6	~6 (5.7) <sup>k</sup>	7.9	$6.6^l$
11	230	190–265	$12.8 \pm 1.0$	$12.8 \pm 1.0$	$5.6 \pm 0.7$	$5.7 \pm 0.7$	~6 <sup>m</sup>	$3.5^m, 5.7^o$	$4.2^l$
12	310	260–380	$12.5 \pm 1.0$	$12.4 \pm 1.0$	$7.3 \pm 0.6$	$7.5 \pm 0.6$	7.3	14.0	$7.9^p$
13	240	203–285	$12.8 \pm 1.0$	$12.8 \pm 1.0$	$6.4 \pm 0.4$	$6.7 \pm 0.4$		$9.1^q, 11.0^r, 12.6^s$	$6.9^l$
15	240	213–285	$13.6 \pm 1.0$	$13.1 \pm 1.0$	$7.0 \pm 0.6$	$6.4 \pm 0.6$		13.4	

<sup>a</sup> Exchange broadening of EPR lines monitored over this range. <sup>b</sup> Subscript f refers to the process QA  $\rightarrow$  QE and subscript b to the process QE  $\rightarrow$  QA. The errors given for  $\log A$  are upper limits, the calculated errors all being ca. 0.1 log unit. The errors on  $E$  correspond to  $2\sigma$ . <sup>c</sup> Free energy barrier for ring-atom site exchange of the corresponding cycloalkane as measured by NMR line broadening. Data are from ref 11 unless otherwise noted. <sup>d</sup> Minimum enthalpic barrier calculated by Dale.<sup>25</sup> <sup>e</sup> Force field calculation of strain energy difference between the transition state and the most stable cycloalkane conformer. <sup>f</sup> Data are for *cis*-(4-methylcyclohexyl)methyl radical<sup>6</sup> because cyclohexylmethyl does not exhibit exchange broadening in the accessible temperature range. <sup>g</sup> Reference 44. <sup>h</sup> Reference 33. <sup>i</sup> Reference 27. <sup>j</sup> Reference 21. <sup>k</sup> Value for 1,1-difluorocycloundecane.<sup>32</sup> <sup>l</sup> Reference 45. <sup>m</sup> Reference 37. <sup>n</sup> Via [1334] and [335]. <sup>o</sup> Via [1343]. <sup>p</sup> Reference 40. <sup>q</sup> For the low-energy triangular conformer **15** via [1345] and [445]. <sup>r</sup> For the two lowest quinquangular conformers **13** and **14** via [12433], [346], [13333], and [347]. <sup>s</sup> For **13** and **14** via [12133]. <sup>t</sup> Reference 41.

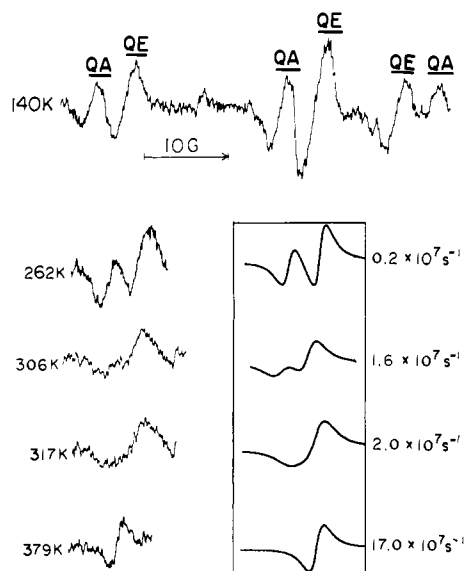


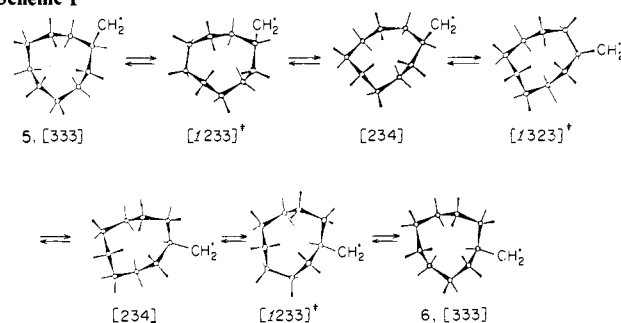
**Figure 5.** EPR spectra (9.4 GHz) of **1** ( $n = 12$ ) at various temperatures. Top: low-field half of spectrum in cyclopropane. Below: lowest field multiplet in *tert*-butylbenzene. Experimental spectra appear on the left; simulated spectra (boxed) appear on the right with rate constants for exchange used in the simulations.

three-jump model, but the spectra are, unfortunately, not sufficiently well-resolved to determine the relative concentrations of the three species involved. Since simulation is impractical, we note only that the coalescence temperature was about 230 K, which implies that the activation energies of both exchange processes are ca. 6 kcal/mol with probably no more than 1 kcal/mol difference between the barriers for the two processes.

**1** ( $n = 11$ ). As reported previously<sup>7</sup> well-resolved spectra of the QA and QE radicals can be observed (Table I). The [QA]/[QE] ratios at low temperatures yielded the van't Hoff parameters listed in Table II. Exchange broadening was successfully simulated with a two-jump model using extrapolated values for the relative concentrations of the two radicals during exchange. The derived Arrhenius parameters are given in Table III.

**1** ( $n = 12$ ). The QA and QE radicals give well-resolved spectra (see Figure 5), and the ratio of their concentrations varies only slightly with temperature, with the QA conformer predominating over the accessible temperature range (see Figure 3). Exchange broadening occurred at rather higher temperatures (260–380 K) than for the cycloalkylmethyl radicals having  $n = 9$ –11, 13, and 15, indicating a higher activation energy for the exchange process of the  $n = 12$  radical. The broadening was successfully simulated with a two-jump model (Figure 5). The derived Arrhenius pa-

#### Scheme I



rameters are given in Table III.

**1** ( $n = 13$ ). The spectra of the QA and QE radicals are well-resolved (see Table I), with the latter predominating throughout the accessible temperature range (Figure 3 and Table II). The exchange broadening observed from 200–290 K was successfully simulated with a two-jump model (Table III).

**1** ( $n = 15$ ). The QA and QE radicals are well-resolved (see Table I), but now it is the QA radical that predominates and its predominance increases as the temperature decreases (see Figure 3), which makes this system unique. The QE radical had a line width slightly greater than that of other QE radicals, which could indicate the presence of more than one kind of QE radical. However, exchange broadening (210–290 K) could be satisfactorily simulated with a two-jump model (Table III).

#### Discussion

**Conformations of Cycloalkylmethyl Radicals.** That **1** ( $n = 6$ ) should exist in two distinct conformations, axial **3** and equatorial **4**, is not surprising. However, that **1** ( $n = 7$  and 8) should appear to exist in only one conformation (probably QA to judge from their  $a^{\text{H}}$  values) is a surprise, while it is quite astonishing that **1** ( $n \geq 9$ ) should exist in just two clearly identifiable conformations (always remembering that **1** ( $n = 10$  and 15) may have two QE conformers, *vide supra* and *infra*). In the following sections we attempt to identify the QA and QE conformations of those **1** having  $n \geq 9$ .

**1** ( $n = 9$ ). The cyclononane conformer of lowest enthalpy is believed to have  $D_3$  symmetry, as in **5** and **6** (see Scheme I). This conformation, which is of the triangular type, has been deduced by Dale<sup>15</sup> using a semiquantitative method of calculation and is designated as [333] by him.<sup>16,17</sup> Following Dale,<sup>15</sup> we use a

(15) Dale, J. *Acta Chem. Scand.* **1973**, *27*, 1115–1129.

(16) Dale's<sup>15</sup> shorthand notation describes the conformation of cyclononane and larger rings in a simple and unequivocal manner. The numbers within the brackets give the number of bonds in one "side", starting with the shortest. The direction around the ring is chosen so that the following number is the smallest possible. A triangular conformation is thus uniquely defined by three numbers.

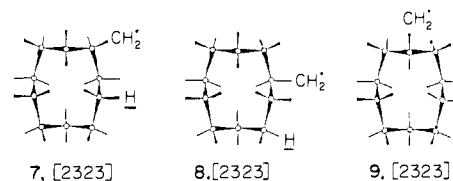
"wedge" representation of the C-C bond, which represents a top-view, perspective drawing. For large rings such drawings are much more convenient than the side-view perspective drawings normally used for cyclohexane rings. The [333] structure has also been deduced to be the most stable form of cyclononane by most force field calculations.<sup>18-21</sup> The [333] structure is also the major conformer present at low temperatures as judged by its <sup>1</sup>H and <sup>13</sup>C NMR spectra,<sup>21,22</sup> but two other conformations cannot be entirely ignored. Thus,<sup>21</sup> at -173 °C, the major conformation (~95%) is [333] and the minor conformation (~5%) is [225], while the third conformation [144] is present only in very small amounts (~1% at -95 °C). However, mainly because [225] has an entropy that is 3.5 eu greater than that of [333], the equilibrium between these conformers is such that, at room temperature, it was estimated<sup>21</sup> that cyclononane contains roughly 40% of the [333], 50% of the [225], and 10% of the [144] conformer. On this evidence, since our experiments were carried out in the temperature range from -176 to -134 °C, only the [333] conformation would be expected to play a significant role.

As has been pointed out,<sup>23</sup> the introduction of a single substituent, such as a CH<sub>3</sub> or CH<sub>2</sub><sup>\*</sup> group, into medium- and large-ring cycloalkanes is not expected to change the stability order of the possible ring conformations, since there will always be on each of these a number of unhindered positions for the substituent. However, a single substituent may lead to a complex mixture of conformers differing only in the position of the substituent on the lowest enthalpy ring conformation(s).<sup>23</sup> On the cyclononane ring in the [333] conformation there are three possible sites for the CH<sub>2</sub><sup>\*</sup> group: the "corner" sites as in **5**; the "outer-edge" sites as in **6**; and the "inner-edge" sites. The last-named sites will be strongly disfavored because of the severe steric crowding that would result. In [333] cyclononane there is only one type of corner site because the axial and equatorial hydrogen atoms are identical; i.e., the corner H atoms are homotopic.<sup>24</sup> Thus, just two conformers of cyclononylmethyl are expected (assuming that the ring is mainly in the [333] conformation at the temperatures of our experiments). Models suggest that the rotation of the CH<sub>2</sub><sup>\*</sup> group will be more hindered when this group is on a corner (by a 1,3-interaction with the H atom on C(3) of the ring) than when it is on an outer-edge site. For this reason, we identify the quasi-axial radical with the larger H<sub>β</sub> hfs as the corner conformer, **5**, and the quasi-equatorial radical as the outer-edge conformer, **6**. Since there are six corner and six outer-edge sites the 5:6 ratio might be expected to be ca. 1.0. Experimentally this ratio is indeed fairly close to unity, there being a slight preference for **6** at T ≤ 110 K and a slight preference for **5** at T > 110 (see Figure 3).

The line broadening observed in the EPR spectra of cyclononylmethyl results from the exchange of corner and outer-edge species, i.e., from the interconversion of **5** and **6**. Dale<sup>25</sup> has shown that interconversion in cyclononane takes place by a "corner migration" via a barrier of the [1233] type to give cyclononane in the [234] conformation.<sup>26</sup> The [234] conformer is then con-

verted to its mirror image via a [1323] barrier and hence via a second [1233] barrier back to the [333] conformer, in which all the carbons have moved one step around the ring, i.e., **5** → **6**. Repetition of this cycle interchanges all ring sites in cyclononane. However, the CH<sub>2</sub><sup>\*</sup> group in the cyclononylmethyl radical cannot adopt inner-edge sites, and so the radical cannot undergo the complete cycle. Interconversion of the CH<sub>2</sub><sup>\*</sup> group occurs by partial cycles ([333] ⇌ [1233]<sup>\*</sup> ⇌ [234] ⇌ [1323]<sup>\*</sup> ⇌ [234] ⇌ [1233]<sup>\*</sup> ⇌ [333]) as shown in Scheme I. Calculations suggest that the [1233]<sup>\*</sup> transition state is the highest energy point on this cycle.<sup>20,21,25,27</sup>

**1** (n = 10). X-ray diffraction studies have shown that the rectangular [2323] conformation (see 7-9) predominates in crystals of several derivatives of cyclodecane.<sup>28,29</sup> The preference



for this conformation has also been confirmed by electron diffraction.<sup>30</sup> The slow-inversion-limit <sup>1</sup>H and <sup>13</sup>C NMR spectra could not be obtained for cyclodecane,<sup>31</sup> but the <sup>19</sup>F NMR spectrum of 1,1-difluorocyclodecane is consistent with the [2323] conformation.<sup>32</sup> Modern force field calculations have also pinpointed [2323] as the lowest enthalpy cyclodecane conformer.<sup>18b,19,30,33,34</sup>

Three cyclodecylmethyl conformers would be expected (7-9). Rotation of the CH<sub>2</sub><sup>\*</sup> group will be most strongly impeded in the corner conformer, **7** (again by a 1,3-interaction with the H atom on C(3) of the ring). We therefore identify **7** as the quasi-axial radical with the large H<sub>β</sub> hfs. When the CH<sub>2</sub><sup>\*</sup> group is on the "short side", i.e. **9**, there will be negligible hindrance to its rotation (the H atoms on C(3) are "round the corner" and about as far removed from CH<sub>2</sub><sup>\*</sup> as is possible). Models suggest that when the CH<sub>2</sub><sup>\*</sup> group is on the "long side", i.e. **8**, there will be only minor steric interaction with the H atom on C(3). We therefore identify both **8** and **9** as giving EPR spectra of the quasi-equatorial type. However, **8** will probably have a slightly larger H<sub>β</sub> hfs than **9**, which provides a rationale for our partial resolution of two QE radicals.<sup>35</sup> On statistical grounds the ratio of concentrations of **7:8:9** would be 8:4:2, i.e., QA:QE ~ 8:6. Experimentally the QA conformers predominate at T ≥ 140 K and the QE conformers predominate at T ≤ 140 K (see Figure 3).

**1** (n = 11). Force field and other calculations have indicated that several cycloundecane conformations have rather similar strain energies.<sup>15,18b,19,36,37</sup> The most recent calculations<sup>37</sup> suggest that the triangular [335] conformer, **10**, may be preferred, although two quinquare conformers, [12323] and [12314], and another triangular conformer, [344], are close in energy. An X-ray diffraction study of cycloundecanone<sup>38</sup> supported **10** as the preferred conformer. The NMR spectra of cycloundecane are also

(17) This conformation is referred to as a "twist boat-chair" by many workers.

(18) (a) For a comprehensive listing of force field calculations on cyclononane see ref 19. (b) This reference also provides an excellent summary of the results obtained by force field calculations, NMR, etc., on the conformations of other cycloalkanes.

(19) Burkert, U.; Allinger, N. L. *Molecular Mechanics*; ACS Monograph 177; American Chemical Society: Washington, DC, 1982; pp 89-108.

(20) The most recent calculations on cyclononane<sup>21</sup> give the following as strain energies (in kcal/mol) relative to the [333] conformation. Energy minima as follows: [333], 0; [144], 1.2; [225], 1.7; [234], 3.2. Conformational transition states as follows: [1323], 4.4; [1224] 6.0; [1233], 7.0; [18], 8.3; [134], 9.9.

(21) Anet, F. A. L.; Krane, J. *Isr. J. Chem.* **1980**, *20*, 72-83.

(22) Anet, F. A. L.; Wagner, J. J. *J. Am. Chem. Soc.* **1971**, *93*, 5266-5268.

(23) Dale, J. *Acta Chem. Scand.* **1973**, *27*, 1149-1158.

(24) Eiliel, E. L. *J. Chem. Educ.* **1971**, *48*, 163-167; **1980**, *57*, 52-55. Because the corner C-H bonds are at equal angles with respect to the plane of the ring, the word "isoclinal" has also been used to describe them. See: Hendrickson, J. B. *J. Am. Chem. Soc.* **1964**, *86*, 4854-4866.

(25) Dale, J. *Acta Chem. Scand.* **1973**, *27*, 1130-1148.

(26) The notation for energy minima<sup>15,16</sup> is expanded<sup>25</sup> to barriers by defining the syn eclipsed bond as a one-bond side; it is marked in italics.

(27) Rustad, S.; Seip, H. M. *Acta Chem. Scand., Ser. A* **1975**, *A29*, 378-380.

(28) Dunitz, J. D. *Pure Appl. Chem.* **1971**, *25*, 495-508.

(29) This conformation has also been referred to as the boat-chair-boat.

(30) Hilderbrandt, R. L.; Wieser, J. D.; Montgomery, L. K. *J. Am. Chem. Soc.* **1973**, *95*, 8598-8605.

(31) Anet, F. A. L.; Cheng, A. K.; Wagner, J. J. *J. Am. Chem. Soc.* **1972**, *94*, 9250-9252.

(32) Noe, E. A.; Roberts, J. D. *J. Am. Chem. Soc.* **1972**, *94*, 2020-2026.

(33) Allinger, N. L. *J. Am. Chem. Soc.* **1977**, *99*, 8127-8134.

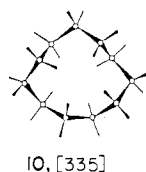
(34) White, D. N.; Bovill, M. J. *J. Chem. Soc., Perkin Trans. 2* **1977**, 1610-1623.

(35) Since calculations suggest that there is at least one other cyclodecane conformation, [1324] (=TCCC), rather close in energy to the [2323] conformation,<sup>19</sup> we cannot rule out the possibility that the second QE radical does not belong to a [2323] structure. However, the low temperatures of our experiments, viz., -145 to -89 °C, make this rather unlikely.

(36) Engler, E. M.; Andose, J. D.; Schleyer, P. v. R. *J. Am. Chem. Soc.* **1973**, *95*, 8005-8025.

(37) Anet, F. A. L.; Rawdah, T. N. *J. Am. Chem. Soc.* **1978**, *100*, 7810-7814.

(38) Groth, P. *Acta Chem. Scand., Ser. A* **1974**, *28*, 294-298.

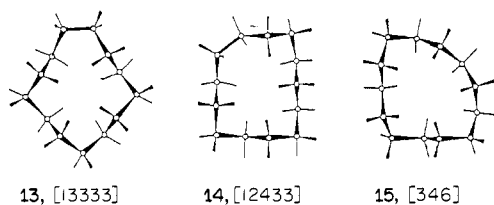


consistent, with **10** being the main species present at low temperatures.<sup>31,37</sup>

The EPR spectral data are readily rationalized in terms of conformer **10**, which would give two distinguishable cycloundecylmethyl radicals: a corner type, which we identify with the QA spectrum (larger  $H_\beta$  hfs), and an outer-edge type, which we identify with the QE spectrum. The statistical ratio of corner to outer-edge sites is 6:8, which is close to the experimental QA:QE ratios (e.g., 0.79 at 140 K; see also Figure 3). Corner and edge positions are interchanged by a type of pseudorotation in cycloundecane,<sup>25,37</sup> but complete pseudorotation is unlikely in the cycloundecylmethyl radical because the  $\text{CH}_2^*$  group is unlikely to be able to occupy an inner-edge site. Nevertheless, corner and outer-edge radicals can exchange by partial pseudorotations.

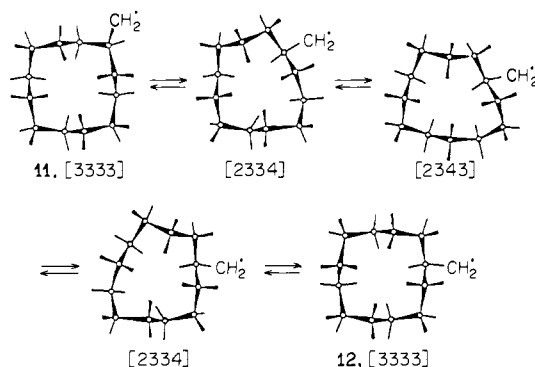
**1** ( $n = 12$ ). The lowest energy conformation of cyclododecane has the symmetrical, quadrangular [3333] structure, **11** and **12**, of  $D_4$  symmetry (Scheme II). This "square" conformation has been found in the crystalline state,<sup>39</sup> is consistent with NMR data,<sup>31,40</sup> and is the one calculated to be of lowest enthalpy by various methods.<sup>15,18b,19,36,40</sup> Other conformations are higher in enthalpy<sup>15,40</sup> and probably will not contribute in the accessible temperature range. The two cyclododecylmethyl radicals are of the corner (homotopic) type, **11**, and outer-edge (equatorial) type, **12**, which we identify as QA and QE, respectively. On statistical grounds, the [11]:[12] ratio would be 1.0; the experimental ratio is 0.6 at 150 K (see Figure 2). The only possible sequence for the exchange of corner and edge positions<sup>25,40</sup> that avoids placing the  $\text{CH}_2^*$  group in an inner site is shown in Scheme II.

**1** ( $n = 13$ ). There are five low-enthalpy conformations of cyclotridecane,<sup>25,37,41</sup> with two quinquangular structures, **13** [13333] and **14** ([12433], and a trinangular, **15** [346], being of lowest energy.<sup>41</sup> The <sup>13</sup>C NMR spectrum of cyclotridecane defied analysis,<sup>41</sup> but an X-ray structure of a 13-membered ring containing nitrogen showed that the main conformer had the [13333] structure.<sup>41</sup>

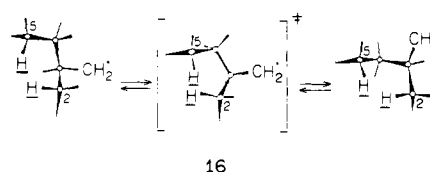


Both the quinquangular conformations have 10 corner sites and 8 outer-edge sites for the  $\text{CH}_2^*$  group, so the corner to edge statistical ratio is 1.25. This ratio is very different from the experimental [QA]:[QE] ratio, e.g., 0.37 at 150 K (see Figure 3). Models indicate that the corner sites next to the one-bond edge are not homotopic. The  $\text{CH}_2^*$  group in these two corners can be in either a pseudoaxial or pseudoequatorial position. In the former position, there would be significant steric hindrance (1,3-interaction) to rotation of  $\text{CH}_2^*$ , but in the latter position, hindrance would be minimal. These particular corner radicals should therefore show distinct EPR spectra, but no "extra" lines could be detected and line widths were normal. While this does not exclude conformations **13** and **14**, since low concentrations of these novel corner radicals might escape detection, it is obvious that our EPR data are in better accord with cyclotridecylmethyl

Scheme II



Scheme III



radicals existing mainly in the triangular conformation, **15**. For this conformer the corner to outer-edge statistical ratio is 0.6, which is much closer to the observed [QA]:[QE] ratios (see Figure 3).

**1** ( $n = 15$ ). Calculations indicate that cyclopentadecane has five low-enthalpy conformations, all of the quinquangular type.<sup>15,37</sup> The [33333] conformer is lowest in enthalpy<sup>15,37</sup> but is entropically disfavored<sup>15</sup> relative to the other four, less symmetric, low-enthalpy conformers, viz., [13443], [13434], [14334], and [13353], and for this reason cyclopentadecane probably exists as a mixture of all five conformers. For any quinquangular cyclopentadecane the statistical corner to outer-edge ratio is 1.0, which is not too different from the experimental [QA]:[QE] ratios (e.g., 2.0 at 150 K, see Figure 2). The four low-energy, one-bond-sided conformers should give rise to novel corner radicals as indicated above for **1** ( $n = 13$ ). The unusually broad lines of the QE radical at the slow-exchange limit might be interpreted as favoring a contribution from these novel corner radicals.

**Dynamics of Corner to Outer-Edge Interconversion of Cycloalkylmethyl Radicals.** The calculated Arrhenius parameters for the  $\text{QA} \xrightarrow{f} \text{QE}$ , corner to outer-edge, interconversions and for the  $\text{QE} \xrightarrow{b} \text{QA}$ , outer-edge to corner, interconversions are given in Table III. The preexponential factors are not sufficiently accurate to warrant detailed discussion. We therefore note only that they are all reasonably close to the expected value of  $10^{13} \text{ s}^{-1}$ . The activation energies of the forward reactions and back-reactions differ because the corner and outer-edge radicals differ in enthalpy. The mean of  $E_f$  and  $E_b$  should be close to the activation energy for ring-atom site exchange in the unsubstituted cycloalkane because a single, small substituent will have little or no effect on these barriers.<sup>11,23</sup>

In the outer edge to corner migration of the  $\text{CH}_2^*$  group, the transition state, **16**, has one torsional angle equal to  $0^\circ$  and the other two equal to  $120^\circ$ <sup>25,37</sup> (see Scheme III). It therefore resembles the syn barrier for the  $n$ -butane internal rotation about the central C-C bond, which has a value of ca. 6 or 7 kcal/mol.<sup>15,36,42</sup> Values of  $E_f$  and  $E_b$  for **1** ( $n \geq 9$ ) are of this general magnitude (see Table III). This is somewhat surprising, as enhanced barriers in the rings might be expected, since the axial hydrogens on C(2) and C(5),  $H$ , cannot avoid each other in the transition state, **16**, as efficiently in rings as in  $n$ -butane. Perhaps this anticipated steric enhancement of the ring barriers is offset by an increase in the C-C-C angles in the rings.

(39) Dunitz, J. D.; Sheaver, H. M. *M. Helv. Chim. Acta* **1960**, *43*, 18-35. Dunitz, J. D. *Perspect. Struct. Chem.* **1968**, *2*, 1-70.

(40) Anet, F. A. L.; Rawdah, T. N. *J. Am. Chem. Soc.* **1978**, *100*, 7166-7171.

(41) Rubin, B. H.; Williamson, M.; Takeshita, M.; Menger, F. M.; Anet, F. A. L.; Bacon, B.; Allinger, N. L. *J. Am. Chem. Soc.* **1984**, *106*, 2088-2092.

(42) Ito, K. *J. Am. Chem. Soc.* **1953**, *75*, 2430-2435. Piercy, J. E.; Rao, M. G. S. *J. Chem. Phys.* **1967**, *46*, 3951-3959. Hoyland, J. R. *Ibid.* **1968**, *49*, 2563-2566. Radom, L.; Pople, J. A. *J. Am. Chem. Soc.* **1970**, *92*, 4786-4795. Radom, L.; Lathan, W. A.; Hehre, W. J.; Pople, J. A. *Ibid.* **1973**, *95*, 643-698.

Since the entropies of activation will probably be small, the free energies of activation,  $\Delta G^\ddagger$ , estimated from the  $^{13}\text{C}$  NMR coalescence temperatures of the cycloalkanes would be expected to be similar to the mean of our values for  $E_f$  and  $E_b$ . Such appears to be the case (see Table III). This table also includes the enthalpic barriers estimated by Dale<sup>25</sup> and barriers calculated by force field methods. Dale's values reproduce the trends we observe experimentally but are generally too high, probably for the reasons he discusses.<sup>25</sup> Our measurements agree reasonably well with the available barriers calculated by force field methods.

### Experimental Section

$^1\text{H}$  and  $^{13}\text{C}$  NMR spectra were recorded on a Bruker WP 80 and a Varian CFT 20 instrument, respectively, in  $\text{CDCl}_3$  at ambient temperature with tetramethylsilane as internal standard. Mass spectra were obtained on an A.E.I. MS 902 spectrometer. EPR spectra were recorded on a Bruker ER 200 D instrument with samples that had been degassed by several freeze-pump-thaw cycles. They were sealed in 4-mm-o.d. Spectrosil tubes and irradiated in the cavity of the spectrometer with light from a 500-W super-pressure mercury arc lamp.

**Methylenecyclononane.** To *n*-butyllithium (65 mL, 1.6 M in hexane) in dry ether (100 mL) under  $\text{N}_2$  was added methyltriphenylphosphonium bromide (23 g), and the solution was stirred for 60 min. Cyclononane (6 g) in ether (30 mL) was added dropwise, and the solution was then refluxed for 10 h. Ether and hexane were distilled off, and glyme (100 mL) was added. The mixture was heated to ca. 85 °C for 4.5 h, cooled in ice, and filtered and the glyme solution extracted with light petroleum ether ( $5 \times 50$  mL). The petroleum extracts were washed with water ( $3 \times 30$  mL), dried over  $\text{Na}_2\text{SO}_4$ , and distilled to give methylenecyclononane: bp  $\sim 110$  °C (20 Torr); 54% yield;  $^1\text{H}$  NMR  $\delta$  1.3–1.9 (6 H, br m), 1.9–2.3 (2 H, br m), 4.85 (2 H, s).

**Cyclononylmethanol.** To methylenecyclononane (3 g) in dry THF (40 mL) cooled in ice was added  $\text{BH}_3$ -THF complex (16 mL). The solution was stirred 30 min, and water (2.3 mL) was added; the mixture was then heated at 45 °C, and 3 M NaOH (12 mL) was added, followed by  $\text{H}_2\text{O}_2$  (5.5 mL of a 30% solution). This mixture was stirred for 60 min and cooled, ether (100 mL) was added, and the mixture was then separated. The aqueous layer was saturated with NaCl and extracted twice with ether. The combined ether extracts were dried and distilled to give cyclononylmethanol: bp  $\sim 180$  °C (20 Torr); 86% yield;  $^1\text{H}$  NMR  $\delta$  1.52 (18 H, br s), 3.42 (2 H, d,  $J = 6$  Hz).

**Cyclononylmethyl Bromide.** Cyclononylmethanol (2.9 g) and triethylamine (1.9 g) in dichloromethane (120 mL) were cooled in ice, and  $\text{CH}_3\text{SO}_2\text{Cl}$  (2.3 g) was added, drop by drop. After the mixture was stirred for 30 min, water was added and the  $\text{CH}_2\text{Cl}_2$  layer was separated, washed with 2 M HCl, brine, and  $\text{NaHCO}_3$  solution, and dried over  $\text{Na}_2\text{SO}_4$ . The  $\text{CH}_2\text{Cl}_2$  was then removed on a rotary evaporator at room temperature. The mesylate was added to LiBr (5.0 g) in dry acetone (65 mL), this mixture was refluxed for 18 h and filtered, and the acetone was removed on a rotary evaporator. The residue was dissolved in light petroleum ether, which was washed with water, dried ( $\text{Na}_2\text{SO}_4$ ), and then chromatographed on a column of silica gel. The bromide was eluted with the first 200 mL of light petroleum ether. It was distilled: bp 78 °C (0.5 Torr); 62% yield;  $^1\text{H}$  NMR  $\delta$  1.51 (17 H, br s), 3.62 (2 H, d,  $J = 6$  Hz);  $^{13}\text{C}$  NMR  $\delta$  23.7, 24.7, 25.2, 30.0, 38.4, 41.8;  $M^+$ (obsd) = 218.0659,  $\text{C}_{10}\text{H}_{19}$   $^{79}\text{Br}$  requires 218.0670.

**Cyclodecylmethyl Bromide.** This was prepared from cyclodecanone by the same method as cyclononylmethyl bromide and was purified in the same way: bp  $\sim 100$  °C (0.5 Torr); 83% yield;  $^1\text{H}$  NMR  $\delta$  1.6 (18 H, s), 1.9 (1 H, m), 3.5 (2 H, d,  $J = 6$  Hz);  $M^+$ (obsd) = 234 and 232.

**Cycloundecylmethyl Bromide.** This was prepared as described previously.<sup>7</sup>

**Methylenecyclododecane.** To a suspension of zinc dust (14.8 g) in  $\text{CH}_2\text{Br}_2$  (13.0 g) and dry THF (250 mL) was added 55 mL of a 1.0 M solution of  $\text{TiCl}_4$  in dichloromethane.<sup>43</sup> The suspension was stirred for 15 min, and then cyclododecanone (9.1 g) in THF (50 mL) was added dropwise and the mixture stirred overnight. The mixture was diluted with ether, and the organic layer was washed with 1 M HCl and brine, then dried ( $\text{Na}_2\text{SO}_4$ ), and chromatographed on alumina after removal of the solvent. The product was distilled: bp 76 °C (0.6 Torr); 70% yield;  $^1\text{H}$  NMR  $\delta$  1.4 (18 H, br s), 1.9–2.2 (4 H, m), 4.80 (2 H, s).

**Cyclododecylmethyl Bromide.** A rapid stream of dry HBr was bubbled through a solution of methylenecyclododecane (2.0 g) and benzoyl peroxide (0.1 g) in light petroleum ether (16 mL) for 30 min at 20 °C. Nitrogen gas was then passed through the solution for 15 min to remove unreacted HBr. The mixture was diluted with light petroleum ether (40 mL), washed with  $\text{NaHCO}_3$  solution, and dried, and the solvent was removed. Crystals of benzoic acid, which separated on standing overnight, were also removed, and the residual oil was distilled: bp 120–122 °C (5 Torr); 90% yield;  $^1\text{H}$  NMR  $\delta$  1.4 (23 H, br s), 3.45 (2 H, d,  $J = 6$  Hz);  $^{13}\text{C}$  NMR, unresolved group of peaks at  $\delta$  20–26, plus singlets at  $\delta$  28.2, 36.7, and 40.0;  $M^+$ (obsd) = 262 and 260.

**Cyclotridecylmethyl Bromide.** Methylenecyclotridecane was prepared from the ketone by the Wittig procedure described above and was converted to the bromide by HBr addition under free-radical conditions, again as described above: bp 92–94 °C ( $10^{-3}$  Torr); 62% yield;  $^1\text{H}$  NMR  $\delta$  1.35 (25 H, br s), 3.35 (2 H, d,  $J = 6$  Hz);  $M^+$ (obsd) = 276 and 274.

**Cyclopentadecylmethyl Bromide.** This was prepared from the ketone by the Wittig reaction, followed by HBr addition to the alkene: bp 120–122 °C ( $10^{-3}$  Torr); 75% yield;  $^1\text{H}$  NMR  $\delta$  1.3 (29 H, br s), 3.30 (2 H, d,  $J = 6$  Hz);  $M^+$ (obsd) = 304 and 302.

**Acknowledgment.** We thank NATO for the award of a research grant, without which the present work would not have been undertaken. J.C.W. thanks the Carnegie Trust for a travel grant. We also thank Dr. I. MacInnes, S. Blake, and L. P. Henry for carrying out some of the experimental work.

**Registry No.** **1** ( $n = 6$ ), 67271-34-5; **1** ( $n = 7$ ), 71880-18-7; **1** ( $n = 8$ ), 83386-44-1; **1** ( $n = 9$ ), 110569-64-7; **1** ( $n = 10$ ), 110569-65-8; **1** ( $n = 11$ ), 83386-45-2; **1** ( $n = 12$ ), 110569-66-9; **1** ( $n = 13$ ), 110569-67-0; **1** ( $n = 15$ ), 110569-68-1.

**Supplementary Material Available:** Table IV giving conformer ratios at various temperatures for **1** ( $n = 6, 9-13, 15$ ) (1 page). Ordering information is given on any current masthead page.

(43) Takai, K.; Hotta, Y.; Oshima, K.; Nozaki, H. *Tetrahedron Lett.* **1978**, 2417–2420.

(44) Wiberg, K. B.; Boyd, R. H. *J. Am. Chem. Soc.* **1972**, *94*, 8426–8430.

(45) Anet, F. A. L.; Cheng, A. K., unpublished results cited in: Dale, J. *Top. Stereochem.* **1976**, *9*, 199–270.